Organic & Biomolecular Chemistry

Accepted Manuscript

ROYAL SOCIETY OF CHEMISTRY

www.rsc.org/obc

Journal Name

ARTICLE

Probing heterobivalent binding to the endocytic AP-2 adaptor complex by DNA-based spatial screening

Received 00th January 20xx,
Accepted 00th January 20xx

DOI: 10.1039/x0xx00000x

www.rsc.org/

F. Diezmann,[a] L. von Kleist[b], V. Haucke[b] and O. Seitz[a]*

The double helical DNA scaffold offers a unique set of properties, which are particularly useful for studies of multivalency in biomolecular interactions: i) multivalent ligand displays can be formed upon nucleic acid hybridization in a self-assembly process, which facilitates spatial screening ii) valency and spatial arrangement of the ligand display can be precisely controlled and iii) the flexibility of the ligand display can be adjusted by integrating nick sites and unpaired template regions. Herein we describe the use of DNA-based spatial screening for the characterization of the adaptor complex 2 (AP-2), a central interaction hub within the endocytic protein network in clathrin-mediated endocytosis. AP-2 is comprised of a a core domain and two, so-called appendage domains, the α- and the β2-ear, which associate with cytoplasmatic proteins required for the formation or maturation of clathrin/AP-2 coated pits. Each appendage domain has two binding grooves which recognize distinct peptide motives with micromolar affinity. This provides opportunities for enhanced interactions with protein molecules that contain two (or more) different peptide motives. To determine whether a particular, spatial arrangement of binding motifs is required for high affinity binding we probed the distance-affinity relationships by means of DNA-programmed spatial screening with self-assembled peptide-DNA complexes. By using trimolecular and tetramolecular assemblies two different peptides were positioned in 2–22 nucleotide distance. The binding data obtained with both recombinant protein in well-defined buffer systems and native AP-2 in brain extract suggests that the two binding sites of the AP-2 α-appendage can cooperate to provide up to 40-fold enhancement of affinity compared to the monovalent interaction. The distance between the two recognized peptide motives was less important provided that the DNA duplex segments were connected by flexible, single strand segments. By contrast, the experiments with a more rigid, duplex-spaced assembly revealed marked distance dependencies. Consequences for the function of adaptor proteins are discussed.

Introduction

The adaptor complex AP-2 plays a key role in assembling the protein interaction network that orchestrates clathrin-mediated endocytosis.[1, 2] The heterotetrameric AP-2 protein complex (consisting of α, β2, μ2, and σ2 subunits) links clathrin to membrane regions destined to form clathrin-coated vesicles. AP-2 harbors binding sites for phosphatidylinositolphosphates, clathrin, and peptide motives found in membrane cargo proteins targeted for internalization via clathrin-mediated endocytosis.[3, 4] Furthermore, AP-2 comprises two ear (also termed appendage) domains, the α-ear and the β2-ear, for interactions with other endocytic accessory proteins such as amphiphysin 1/2, intersectin 1/2, β-arrestins, synaptojanin 1-p170 (SJ170), epsins, and Eps15 among others (Figure 1).[5-8] Each ear domain contains two binding sites; the so-called top sites and the side sites, which recognize differing peptide motives in the unfolded regions of the accessory proteins. Clathrin is recruited to membrane-bound AP-2, e.g. via interactions with a peptide motiv within the β-hinge region among other interactions.

Owing to the multitude of binding opportunities the AP-2 complex serves as a heteromultivalent interaction hub. This provides a means for affinity enhancements when different AP-2 binding sites are simultaneously targeted by proteins that contain two or more different types of peptide motifs. As a result, the collective binding properties of the AP-2 interaction sites critically determine functional properties of the adaptor protein during clathrin-mediated endocytosis. For example, cooperative behaviour should facilitate bimolecular protein-protein interactions at low concentration of AP-2 and/or the binding partner. We decided to probe the distance-affinity relationships governing heterobivalent interactions with AP-2. Such relationships determine whether a particular, spatial arrangement of binding motifs is required for high affinity binding and should, therefore, be critical for the selection of binding partners during clathrin-mediated endocytosis.

[a] Humboldt-Universität zu Berlin, Institut für Chemie, Brook-Taylor-Str. 2, D-12489 Berlin, Germany.
[b] Freie Universität Berlin, Department of Biology, Chemistry and Pharmacy and Leibniz Institut für Molekulare Pharmakologie (FMP), Robert-Rössle-Strasse 10, D-13125 Berlin, Germany.

Electronic Supplementary Information (ESI) available: Details on the synthesis of peptides, oligonucleotides, peptide nucleic acids, oligonucleotide-peptide conjugates and recombinant GST-fusion protein, characterization data, and binding assays. See DOI: 10.1039/x0xx00000x

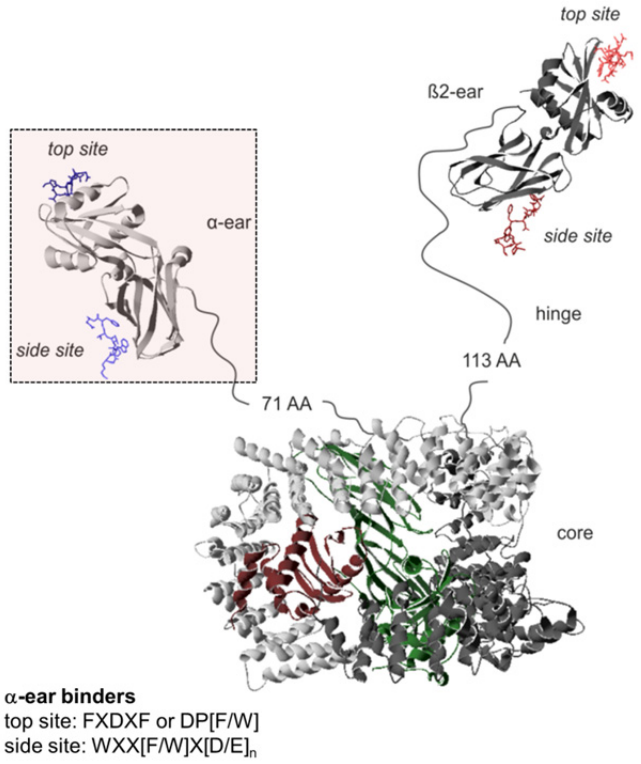

Figure 1. Graphical representation of the heterotetrameric adaptor protein AP-2 comprised of a core domain and two appendage domains (α ear and β2 ear) in complex with peptides that bind to the top and side sites of the ear domains (model based on pdb entries 2VGL, 2VJO, 2G30 and 3HS9).

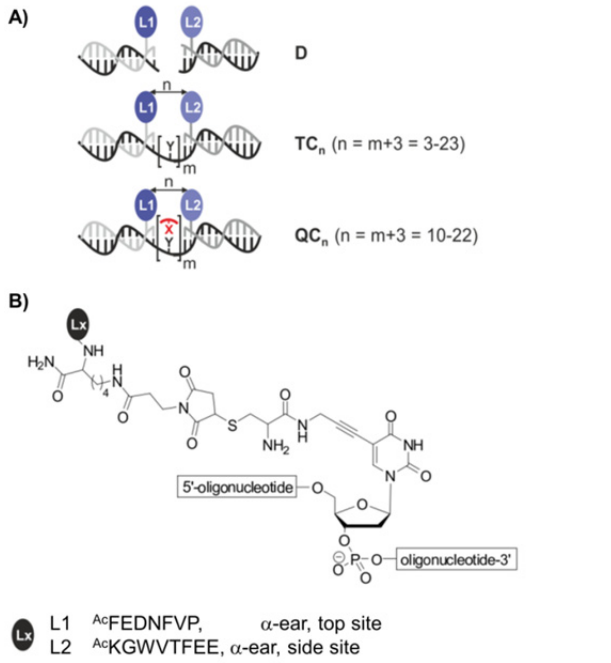

Figure 2. A) Peptide-DNA complexes used for DNA-based spatial screening of the AP-2 α-ear: duplex DNA (**D**), ternary DNA complexes (**TC$_n$**) and quaternary DNA complexes (**QC$_n$**). B) Chemical structure of peptide-DNA linkage and peptide ligands and cognate binding sites. See Table S2 for sequences of oligonucleotides used.

Owing to their important role in recruiting other endocytic proteins to the plasma membrane we selected the ear domains of AP-2, which are connected to the central AP-2 core via flexible 71 and 113 amino acid long hinge regions. It has been shown that proteins capable of occupying both binding sites bind the α-appendage with higher affinity than proteins targeting only a single binding site.[5, 8, 9] However, a distance-affinity study has not been reported.

We made use of a tailor-made multivalent probe system, which allows control over both the valency and the spatial arrangement of the ligand display. Ideally, such a probe system shall provide information about i) the extent of affinity enhancements achievable by concurrent interactions and ii) the distance between the binding motives.[10-12] We and others have previously shown that the double helical DNA scaffold offers a unique set of properties, which are particularly useful for studies of multivalency in biomolecular interactions.[13-29] For example, nucleic acid-programmed ligand displays have been used to provide for high affinity binding to thrombin,[29] adaptor proteins,[24] antibodies,[19, 23, 28] and cell surface receptors[22, 26, 27] as well as to measure the distance between binding sites in lectins,[16, 17, 20] tandem SH2 domains,[15] estrogen receptor[13] and the X-linked inhibitor of apoptosis protein[14]. Based on this, we decided to apply DNA-programmed spatial screening to the characterization of heterobivalent interactions of the AP-2 α-ear domain. This study also included the development of a binding assay, by which the interactions between AP-2 and DNA self-assemblies can be studied in tissue lysates.

Results

Design

The DNA-programmed spatial screen involved DNA complexes (Figure 2A) which were designed to present two different peptides for simultaneous interactions with the AP-2 ear domains. The ternary complexes **TC$_n$** are comprised of two 15 nt long peptide-DNA conjugates and a 30-50 nt long DNA template. The template strands used for annealing of the peptide-DNA conjugates featured a segment that remained unpaired upon formation of the complexes **TC$_n$**. This single-stranded region provides for flexibility, which may facilitate simultaneous interactions with the top and side sites across the convex protein surface. For a more defined peptide display we, for the first time, considered the use of DNA- or peptide nucleic acid (PNA)-based rigidifier strands. The unpaired spacer regions were hybridized with equally long, complementary DNA or PNA strands (red in Figure 2A), yielding quaternary complexes **QC$_n$**. The two nick sites in **QC$_n$** serve as hinges, which, in analogy to the nicks installed by DNA-topoisomerases, provide rotational degrees of freedom. The semiflexible complexes **TC$_n$** and the rigidified complexes **QC$_n$**, were designed for ligand presentation up to 80 Å distance.

Selection of peptide binders.

The α-ear domain was recombinantly expressed in E. coli as GST fusion protein and a fluorescence anisotropy assay was

used to identify peptide binders that provided suitable micromolar affinity for one of the binding sites (Table 1). The top site of the α-ear binds to Dx[F/W] and with a higher affinity to extended FxDxF consensus sequences.[6, 30] From the 5 top site binders (**1**-**5**) evaluated we selected peptide **2** (= **L1**) for further studies owing to its high binding affinity and small size. The screening for optimal binders of the side site involved six peptides (**6**-**11**) comprising the known WXXF consensus.[8, 9, 31] We found that peptides containing acidic residues next to the C-terminal of the consensus provided high binding affinity and selected **8** (=**L2**) for further usage.

Table 1. K_D-values for the interaction of peptides with α-ear appendage of AP-2.

	Peptide sequence[1]	source	Binding	K_D [μM][2]
1	^{Ac}SDPFK(FAM)	Eps15	top site	~ 120
2	^{Ac}FEDNFVPK(FAM), **L1**	amphiphysin	top site	2.1
3	^{Ac}INFFEDNFVPEIK(FAM)	amphiphysin	top site	2.6
4	^{Ac}INFFEDDFVPEIK(FAM)	amphiphysin	top site	5.4
5	^{Ac}LDGFEDNFNLQSK(FAM)	SJ 170	top site	7.6
6	^{Ac}PNNWADFSK(FAM)	intersectin	side site	16.0
7	^{Ac}PNNWADFSSTWPK(FAM)	intersectin	side site	6.5
8	^{Ac}KGWVTFEEK(FAM), **L2**	SJ 170	side site	3.7
9	^{Ac}WVTFDDDK(FAM)	SJ 170	side site	3.5
10	^{Ac}NPKGWVTFEEEEK(FAM)	SJ 170	side site	3.3
11	^{Ac}ISNWVQFEDDTPK(FAM)	stonin	side site	5.5

[1] The consensus motifs are underlined. [2] determined by measurements of fluorescence anisotropy upon titration of the fluorescein-labeled peptides with the recombinant α-appendage.

Spatial screening of the recombinant α-ear domain

The peptides were attached to the oligonucleotides by means of a previously reported thioether ligation, which involved maleimido groups (rather than fluorescein used for peptides in Table 1) at the side chain of a C-terminal lysine residue and cysteinylaminopropargyl-functions protruding from the 5-position of thymidine (Figure 2B).[15, 32] Thermal denaturation analyses showed that the peptides had a negligible influence on the stability of the DNA duplexes (Figure S1). A T_M > 60°C suggested that the complexes maintain their integrity during the binding experiments. For targeting of the α-ear top site the peptide **L1** was attached to an oligonucleotide 15-mer. The side site was targeted by a conjugate, which presented the peptide **L2.** The affinity of DNA-peptide constructs for the α-ear domain was assessed in a competition assay by measuring the displacement of the FAM-labeled reference binder Ac-KGWVTFEEK(FAM), **8**.

The mixture of the two monovalent duplexes **D** provided a reference point for monovalent binding (IC_{50} = 20 μM). Most of the heterobivalent DNA-peptide constructs **TC_n** showed an enhanced protein affinity characterized by an approximately 10-fold increase in the ability to displace the reference peptide **8** from the complex with the α-ear domain (Figure 3A). This suggests that the combined action of both the top site and the side site enables affinity enhancements. The influence of the spacer sequence (oligo-T in **$TC1_n$** vs. mixed sequence in **$TC2_n$**, see Table S2 for sequence information) was negligible.

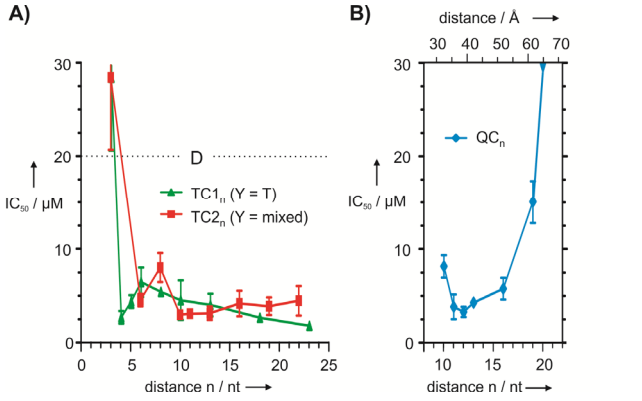

Figure 3. Distance dependent heterobivalent binding of A) ternary peptide-DNA complexes **TC_n** or B) PNA-rigidified complexes **QC_n** to the AP-2 α-ear. The dashed line in Figure 3A marks the affinity determined for a mixture **D** of two monovalent duplexes.

Furthermore, the length of the unpaired segment between den duplex segments in **TC_n** played a minor role. Yet, it was required that the distance between the peptide anchor sites exceeded 3 nucleotides.

For a more precise mapping of distance-affinity relationships, we used rigidifier strands to form complexes **QC_n** (Figure 2A, see also Figure 4A). The T_M of the rigidifier-template complex should be high to maintain the constraints at low concentration. We compared DNA- and PNA-based rigidifiers (Figure S2). Melting analyses revealed the advantages provided by PNA, which has higher affinity for complementary nucleic acid strands than DNA or RNA.[33, 34] A PNA 13-mer was annealed to the middle segment of a 43 nt long DNA template that was used for the construction of **$TC2_{16}$** (Figure 4A). The resulting PNA-DNA duplex showed a T_M > 75°C (Figure 4B). By comparison, the DNA-DNA duplex formed upon hybridization with a sequence identical DNA 13-mer had significant lower stability (T_M > 55°C). Of note, with PNA a 7-mer was sufficient to achieve a TM > 60°C whereas the corresponding 7 nt long oligonucleotide provided a T_M < 45°C (Figure S2A). We, therefore, used PNA-based rigidifiers for the construction of the complexes **QC_n**. The protein affinity measurements with **QC_n** exposed a preferred 11-13 nucleotide distance between the peptide appendage sites. Of note, the best binder **QC_{12}** was 10-fold more potent in binding the AP-2 α-ear domain than complex **QC_{20}**. The latter apparently presented the peptides in a distance too large for simultaneous interactions with both the top site and the side site. An estimate of the distance between the peptide anchor sites considers the 3.25 Å rise per base pair in the PNA-DNA segment (as opposed to a 3.4 Å rise in B-DNA).[35] Given this assumption, the optimum of 11-13 nt between the peptide anchor points corresponds to a distance of approx.. 36-43 Å. Crystal structure analysis showed that the amino acid residues used for conjugation with DNA span a distance of 40-45 Å (Figure S4).[1, 6] This is a noteworthy agreement given the length and flexibility of the linkers that connect the peptide with the DNA part.

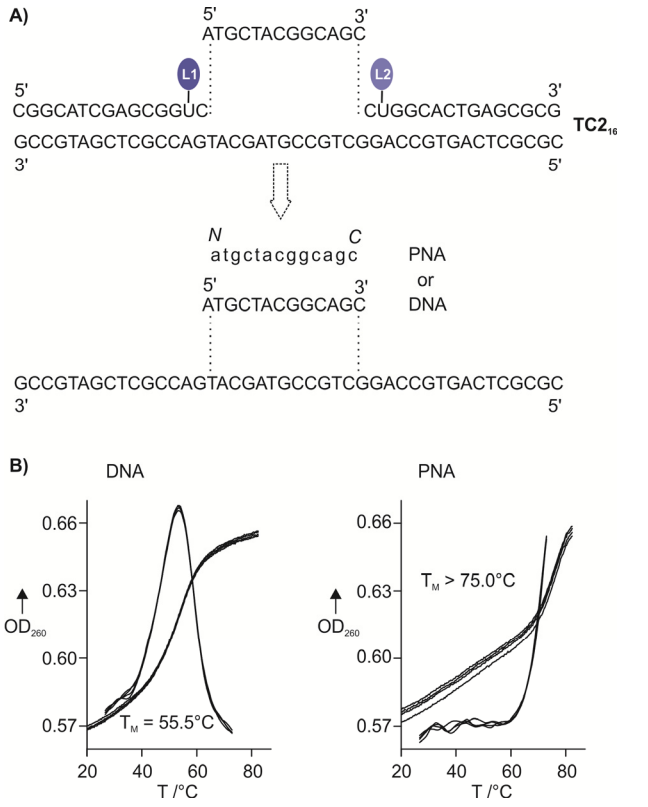

Figure 4. A) Principle for the rigidification of ternary DNA complexes such as **TC2$_{16}$** by annealing of rigidifier strands to the single stranded middle segment. B) Thermal melting analysese of duplexes formed upon hybridization of the 43 nt long DNA template with 13 nt long DNA (left) or PNA (right) oligomers. Conditions: 1 µM oligomers (PNA or DNA) in buffer (10 mM NaH_2PO_4, 100 mM NaCl, pH 7.0)

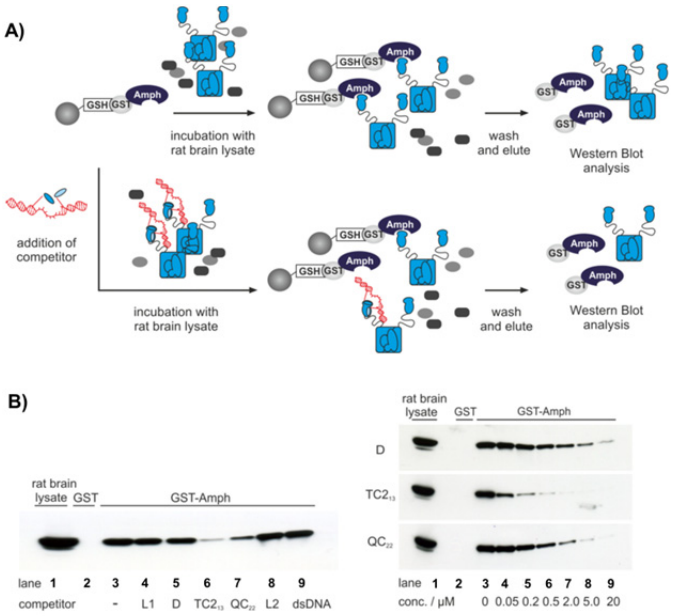

Figure 5. A) AP-2 pull-down assay. A GST-amphiphysin fusion protein was linked to GST-bind resin and used as a bait to capture AP-2 in rat brain extract either in absence (upper part) or presence (lower part) of a competitor. After washing captured proteins are eluted and analyzed by Western Blotting with an antibody (AP50) against the µ2 domain of AP-2 B) Inhibition of AP-2-amphiphysin interaction with peptide-DNA complexes (such as **TC$_{13}$**) targeted against adjacent binding sites within the α-ear domain. Conditions: 25 µg GST or GST-Amph, 0.5 mL of 5.0 mg/mL rat brain lysate, 1 h incubation, buffer: 20 mM HEPES, pH 7.4, 50 mM NaCl, 2 mM $MgCl_2$, 1% TritonX-100, 1 mM PMSF.

Binding of the α-ear domain within full length AP-2 from brain tissue

We next explored the potential for heterobivalent binding of the AP-2 α-ear domain in the context of the full length AP-2 protein in a more challenging matrix. As yet, full-length AP-2 comprising the core and ear domains cannot be expressed in bacteria and is very sensitive to purification procedures as it tends to precipitate at micromolar concentrations. We used rat brain lysate as a source for native AP-2 and developed a pull-down assay to evaluate binding interactions within this complex biomacromolecular environment. GST-tagged amphiphysin 1 (Amph) binds to the α-ear of AP-2 and, following immobilization, was used as a bait protein (Figure 5A). After washing and denaturation-induced elution, the released AP-2 was analyzed by immunoblot analysis. The use of a specific antibody against the µ2 subunit of AP-2 demonstrated the integrity of the captured AP-2. Binders of the α-ear that will be added to the rat brain lysate will compete with immobilized amphiphysin 1 for binding to AP-2 and, depending on the binding affinity, reduce the AP-2 specific signals in the immunoblot.

A specificity control showed that GST alone cannot capture AP-2 (lane 2, Figure 5B). The top site- and side site-specific peptides **L1** and **L2** (lane 4 and lane 8, respectively) were added in 1 µM concentration to the rat brain lysate, but proved inefficient in inhibiting Amph-AP-2 complex formation. Likewise, a mixture of the monovalent, disconnected peptide-DNA conjugates **D** failed in reducing AP-2 binding (lane 5). A strong inhibition of the Amph-AP-2 interaction was achieved when the heterobivalent peptide-DNA conjugate **TC2$_{13}$** was used (lane 6). As expected from the measurements on the purified α-ear domain the PNA-rigidified complex **QC$_{22}$** (lane 7) was a less potent inhibitor than **TC2$_{13}$**.

The inhibitory activity of the DNA-peptide conjugates was evaluated in a dilution series (0.05 – 20 µM inhibitor concentration, Fig. 5B right). Prior to immunoblot analysis the gel was stained reversibly with Ponceau S, which assured that the experiments were performed with identical amounts of GST-Amph (Figure S5B). The monovalent peptide-DNA conjugates **D** showed rather modest inhibition of the Amph-AP-2 interaction. A faint AP-2 signal was still detectable at 20 µM. By contrast, addition of the bivalent complex **TC2$_{13}$** caused a similar reduction of the AP-2 signal already at 0.5 µM. We infer that heterobivalent binding conferred an approx. 40-fold enhancement of the AP-2 binding affinity. The rigidified complex **QC$_{22}$** arranges the peptides in a distance too large for simultaneous binding to the top- and side-sites of the α-ear. This explains why its inhibitory activity was decreased by one order of magnitude in comparison to **TC2$_{13}$**. These results show that bivalency is a necessary but not a sufficient criterion to obtain high affinity binders for the AP-2 α-ear. As found earlier, the spatial arrangement of the ligands on nucleic acid

scaffolds is important when the targeted receptor binding sites are bridged by rigid linkers.[13, 15-18, 23-25]

Discussion

The data from fluorescence polarization detected binding assays and pull-down assays shows that the two binding sites of the AP-2 α-ear domain (top site and side site) can act in concert. The cooperative interaction enabled up to 40-fold enhancement of binding affinity. As a result, a protein or a protein assembly that contains consensus binding motives for both the top site and the side site will be more readily recruited by AP-2 than a "monovalent" protein. Of note, this behaviour has been reported in a qualitative study which described that immobilized full length SJ170 containing both the top site and the side site consensus motive captured a higher amount of AP-2 than a truncated version harboring only a single interaction motif.[8] Likewise, epsin1 and eps15 have been reported to capitalize on the engagement of both binding sites of the α-appendage.[5] Our DNA-programmed spatial screen showed that the heterobivalent complexes **TC_n** showed high affinity for the AP-2 α-ear regardless of the length of the unpaired spacer segment. This suggests that the distance between the two consensus sequences recognized is less important provided that the connecting linker is flexible. This behavior resembles a noteworthy investigation from Whitesides et al. who suggested that flexible linkers that are longer than the required spacing of the binding sites on an rigid target still confer remarkable binding enhancements mainly due to entropic reasons, because the linker can maintain conformational mobility also in the bound form.[36] It is, therefore, plausible to assume that affinity enhancements can be achieved by proteins in which the two interaction motives are part of a structurally disordered region. In contrast, structured proteins would be expected to show a different behaviour. The spatial screening with the rigidified complexes **QC_n** suggests that in such a case affinity enhancements would only be obtainable when the two consensus motives are separated by approx. 36-43 Å.

Conclusions

Herein we described the use of DNA-programmed spatial screening for the characterization of heterobivalent recognition of the heterotetrameric adaptor complex 2 (AP-2), a central interaction hub within the endocytic network in clathrin mediated endocytosis. We explored the potential for synergistic interactions with the two binding grooves in the α-appendage domain, which along with the β2-appendage are required to associate AP-2 with cytoplasmatic proteins during formation or maturation of clathrin/AP-2 coated pits. Peptides with high affinity for the binding grooves were conjugated with DNA strands and arranged in varied distances by means of DNA self-assembly based on duplex formation. The binding data suggests that the two binding sites of the AP-2 α-appendage can cooperate to provide up to 40-fold enhancement of affinity compared to the monovalent interaction. The distance between the two recognized peptide motives was less important provided that the DNA duplex segments were connected by flexible, single strand segments. By contrast, the experiments with a more rigid, duplex-spaced assembly revealed marked distance dependencies. We infer that accessory proteins destined to bind to the AP-2 α-ear should be structurally disordered or, when folded, present the consensus motives in 36-43 Å distance. The difference in binding behaviour i.e. pronounced distance-affinity relationships for structured binding partners versus rather distance-independent binding for less ordered molecules highlights one of the advantages provided by DNA-based scaffolds. The degree of structural order can readily be adjusted from rather flexible complexes such as single-strand-spaced ternary complexes **TC_n** to the PNA-constrained quaternary complexes **QC_n**. Of note, in addition to measurements of recombinant protein in well-defined buffer we also characterized heterobivalent recognition by native full length AP-2 in brain extract. The heterobivalent DNA-scaffolded peptide display remained active in this challenging environment and outcompeted the monovalent interaction between AP-2 and amphiphysin, a known protein binder to the AP-2 α-ear domain. Based on this, we are confident that DNA-based spatial screening is a suitable tool for the interrogation of intracellular protein-protein interactions.

Experimental

Binding assays with recombinant protein

For the determination of K_D-values, a solution of the FAM-labeled peptide (100 nM) in buffer (20 mM HEPES, 50 mM NaCl, 3 mM EDTA, 0.05% CHAPS, pH 7.4, 25°C) in a 0.25 mL fluorescence cuvette was titrated with a 70 µM stock solution of GST-α-ear in buffer, which contained 100 nM peptide. The fluorescence anisotropy was determined before and after each titration step by using a Spex Fluoromax-3 fluorescence spectrometer from Horiba, Jobin Yvon. FAM was excited at 485 nm and the emission was measured at 525 nm. The titration was continued after equilibration of the signals. Fluorescence anisotropy values were normalized and fitted to the equation for a single site-binding isotherm with receptor depletion (Equation 8.10 in Invitrogen Fluorescence Polarization Technical Resource Guide, 3rd edition, Invitrogen Corporation, Madison, 2004).

The affinity of DNA-peptide conjugates for the GST-α-ear was assessed by means of IC_{50}-values. The FAM-labeled peptide **8** was used as a reference binder. A 100 nM solution (150 µL) of this peptide in buffer (20 mM HEPES, 50 mM NaCl, 3 mM EDTA, 0.05% CHAPS, pH 7.4) was added to a 0.25 mL fluorescence cuvette and the fluorescence anisotropy was measured. The resulting value corresponds to the unbound reference peptide. The GST-α-ear was added to a final 2 µM concentration. The measured fluorescence polarization provided the starting value. The peptide-DNA conjugates **D**, **TC_n** or **QC_n** (see Table S2 for sequences) were added from 2

µM, 50 µM or 500 µM stock solutions in buffer (20 mM HEPES, 50 mM NaCl, 3 mM EDTA, 0.05% CHAPS, 100 nM peptide 8, 2 µM GST-α-ear, pH 7.4) to 5 nM to 25 µM final concentration. For the preparation of DNA complexes the required conjugates and oligonucleotides were mixed in buffer containing 100 nM reference binder **8**, heated to 75°C and cooled down slowly (1°C/min) before protein was added. The fluorescence anisotropy was determined before and after each titration step by using a Spex Fluoromax-3 fluorescence spectrometer from Horiba, Jobin Yvon. FAM was excited at 485 nm and the emission was measured at 525 nm. The titration was continued after equilibration of the signals. The normalized anisotropy was plotted against the logarithmic concentration of the peptide-DNA conjugates. Data analysis was performed by using a sigmoidal dose response model with variable slope. The IC_{50} values were determined as the average of three independent measurements.

Pull-down assay

For the preparation of the bait, the E.coli expression strains BL21 and ER2566 carrying the pGEX 4T-1 expression vector with the GST-amphiphysin 1 B/C insert (amino acids 250-578) were used. LB/ampicillin-medium (50 mL, 0.5 % [w/v] yeast extract, 1 % [w/v] trypton, 0.5 % [w/v] NaCl, pH 7.2 50 µg/mL ampicilin) was inoculated with a pipette tip of the bacterium glycerol stock and gently shaken at 37°C and 200 rpm overnight. The overnight culture was diluted (1:20) in selective 2xYT-medium (1 % [w/v] yeast extract, 1.6 % [w/v] trypton, 0.5 % [w/v] NaCl, pH 7.2) and incubated by shaking at 37°C until the OD600 reached 0.7 to 0.8. Protein expression was induced by adding isopropyl-β-D-thiogalactopyranoside (IPTG) to a final concentration of 0.5 mM. The culture was grown for 4 h at 30°C. The bacteria were harvested by centrifugation at 4000 x g for 15 min at 4°C. A cell pellet from a 500 mL culture of GST-amphiphysin was suspended in 20 mL ice-cold PBS and frozen in 4 mL aliquots. The cells of such an aliquot were sonicated by using a Microtip System Sonopuls from Bandelin (Berlin, Germany) for 90 s using 70 % power and 50 % duty cycle. The samples were centrifuged for 15 min at 17,000 x rpm at 4°C. The supernatant was added to pre-washed GST-binding resin (Novagen, 0.5 ml slurry per 500 ml expression culture) and incubated for 2 h at 4°C. The suspension was centrifuged at 2000 x g at 4°C for 2 min and beads were washed three times with PBS. The resulting GST-amphiphysin loaded beads were suspended in 1 ml PBS and used immediately in pull-down assays. The protein concentration was determined by a Bradford assay.

Rat brain lysates were prepared as previously described.[37] The total protein concentration was determined by Bradford assay. The protein concentration was adjusted by addition of buffer (20 mM HEPES, pH 7.4, 50 mM NaCl, 2 mM $MgCl_2$, 1% TritonX-100). To the diluted rat brain lysate 1 mM PMSF and mammalian protease inhibitor cocktail (Sigma; 7 µL/mL) was added. If required, a competitor (peptide, DNA or peptide-DNA in buffer) was added to the prepared rat brain extract. The resulting mixture (0.5 mL) was incubated with GST fusion protein coupled to GST-binding resin (25 µg) for 1 h at 4°C on a rotation wheel. GST alone bound to glutathione coupled beads was used as a negative control. After centrifugation at 2000 x g for 1 min and 4°C, the supernatant was removed and the beads were washed three times with 600 µL buffer (20 mM HEPES, pH 7.4, 50 mM NaCl, 2 mM $MgCl_2$, 1% TritonX-100) and once with 600 µL buffer without Triton-X-100 (20 mM HEPES, pH 7.4, 50 mM NaCl, 2 mM MgCl2). Afterwards, the washing buffer was completely removed using a Hamilton pipette and proteins bound to the beads were eluted by addition of 50 µL of SDS loading buffer (50 mM Tris-HCl, pH 6.8, 100 mM DTT, 2% [w/v] SDS, 0.1% bromphenolblue, 10% [v/v] glycine). The eluates were incubated at 95°C for 5 min and 25 µL aliquots were analyzed by an 8% SDS-PAGE. Electrophoresis was performed in 1 x SDS-PAGE running buffer (24.6 mM Tris, pH 8.8, 0.192 M glycine, 0.1% [w/v] SDS) at 20 mA per gel. For the immunoblotting, proteins were transferred from the polyacrylamide gel to a nitrocellulose membrane by semi-dry electroblotting. A stack of (bottom-to-top) three layers of Whatman paper, the nitrocellulose membrane, the polyacrylamide gel, and another three layers of Whatman paper was assembled in a blotting chamber. All layers were soaked with blotting buffer (20 mM Tris-HCl, pH 8.8, 154 mM glycine, 0.08% SDS, 10% MeOH) and electrotransfer was performed at 1 mA/ cm2 (45 mA per gel). To visualize proteins, the nitrocellulose membrane was stained with Ponceau S (0.2% [w/v] Ponceau S, 1% [v/v] acetic acid in water) for 5 min (Fig S7B). Unspecific staining was eliminated by washing with 1 % acetic acid and the blot was scanned for documentation. To remove residual acidic acid the membrane was washed once with TBS and then cut to allow for several antibody incubations simultaneously. After incubation in blocking buffer (4% milk in TBS) for 1 h at room temperature, the membrane was washed three times with TBS for 5 min. The membrane was incubated with a solution of primary antibody against AP-2 µ2-domain (AP50, monoclonal mouse IgG1, BD Bioscience, Franklin Lakes, USA) diluted in TBS containing 1% BSA and 0.02% NaN3, diluted 1:250 overnight at 4°C. After three 5 min washes in TBS the membrane was exposed to horseradish peroxidase (HRP)-conjugated goat anti-mouse secondary antibodies (diluted 1:5000 in blocking buffer) for 1 h at room temperature. The nitrocellulose membrane was washed three times with TBS and antibodies were detected using the enhanced chemoluminescence (ECL) detection reagent (Amersham Biosciences). The resulting luminescence signals were detected by exposing the membrane to a chemoluminescence film (HyperfilmTM ECL, Amersham Biosciences). The film was developed by incubation in developer and fixation solutions and scanned for documentation

Acknowledgements

This work was supported by the Deutsche Forschungsgemeinschaft (SFB 765).

Notes and references

1. B. M. Collins, A. J. McCoy, H. M. Kent, P. R. Evans and D. J. Owen, *Cell*, 2002, **109**, 523-535.
2. D. J. Owen, B. M. Collins and P. R. Evans, *Annu. Rev. Cell Dev. Biol.*, 2004, **20**, 153-191.
3. L. M. Traub, *Nat. Rev. Mol. Cell. Biol.*, 2009, **10**, 583-596.
4. Y. Rao, C. Rueckert, W. Saenger and V. Haucke, *Eur. J. Cell Biol*, 2012, **91**, 226-233.
5. G. J. K. Praefcke, M. G. J. Ford, E. M. Schmid, L. E. Olesen, J. L. Gallop, S. Y. Peak-Chew, Y. Vallis, M. M. Babu, I. G. Mills and H. T. McMahon, *EMBO J.*, 2004, **23**, 4371-4383.
6. T. J. Brett, L. M. Traub and D. H. Fremont, *Structure*, 2002, **10**, 797-809.
7. D. J. Owen, Y. Vallis, B. M. F. Pearse, H. T. McMahon and P. R. Evans, *EMBO J.*, 2000, **19**, 4216-4227.
8. A. Jha, N. R. Agostinelli, S. K. Mishra, P. A. Keyel, M. J. Hawryluk and L. M. Traub, *J. Biol. Chem.*, 2004, **279**, 2281-2290.
9. S. K. Mishra, M. J. Hawryluk, T. J. Brett, P. A. Keyel, A. L. Dupin, A. Jha, J. E. Heuser, D. H. Fremont and L. M. Traub, *J. Biol. Chem.*, 2004, **279**, 46191-46203.
10. M. Mammen, S. K. Choi and G. M. Whitesides, *Angew. Chem. Int. Ed.*, 1998, **37**, 2755-2794.
11. L. L. Kiessling, J. E. Gestwicki and L. E. Strong, *Angew. Chem. Int. Ed.*, 2006, **45**, 2348-2368.
12. C. Fasting, C. A. Schalley, M. Weber, O. Seitz, S. Hecht, B. Koksch, J. Dernedde, C. Graf, E. W. Knapp and R. Haag, *Angew. Chem. Int. Ed.*, 2012, **51**, 10472-10498.
13. F. Abendroth, A. Bujotzek, M. Shan, R. Haag, M. Weber and O. Seitz, *Angew. Chem. Int. Ed.*, 2011, **50**, 8592-8596.
14. F. Abendroth and O. Seitz, *Angew. Chem. Int. Ed.*, 2014, **53**, 10504-10509.
15. H. Eberhard, F. Diezmann and O. Seitz, *Angew. Chem. Int. Ed.*, 2011, **50**, 4146-4150.
16. C. Scheibe, A. Bujotzek, J. Dernedde, M. Weber and O. Seitz, *Chem. Sci.*, 2011, **2**, 770-775.
17. C. Scheibe, S. Wedepohl, S. B. Riese, J. Dernedde and O. Seitz, *ChemBioChem*, 2013, **14**, 236-250.
18. K. Matsuura, M. Hibino, T. Ikeda, Y. Yamada and K. Kobayashi, *Chem. Eur. J.*, 2004, **10**, 352-359.
19. D. Holowka, D. Sil, C. Torigoe and B. Baird, *Immunol. Rev.*, 2007, **217**, 269-279.
20. M. Ciobanu, K.-T. Huang, J.-P. Daguer, S. Barluenga, O. Chaloin, E. Schaeffer, C. G. Mueller, D. A. Mitchell and N. Winssinger, *Chem. Commun.*, 2011, **47**, 9321-9323.
21. F. Diezmann and O. Seitz, *Chem. Soc. Rev.*, 2011, **40**, 5789-5801.
22. K. Gorska, J. Beyrath, S. Fournel, G. Guichard and N. Winssinger, *Chem. Commun.*, 2010, **46**, 7742-7744.
23. K. Gorska, K.-T. Huang, O. Chaloin and N. Winssinger, *Angew. Chem. Int. Ed.*, 2009, **48**, 7695-7700.
24. R. Liu, B. Jiang, H. Yu and J. C. Chaput, *ChemBioChem*, 2011, **12**, 1813-1817.
25. B. A. R. Williams, C. W. Diehnelt, P. Belcher, M. Greving, N. W. Woodbury, S. A. Johnston and J. C. Chaput, *J. Am. Chem. Soc.*, 2009, **131**, 17233-17241.
26. A. V. Dix, S. M. Moss, K. Phan, T. Hoppe, S. Paoletta, E. Kozma, Z.-G. Gao, S. R. Durell, K. A. Jacobson and D. H. Appella, *J. Am. Chem. Soc.*, 2014, **136**, 12296-12303.
27. E. A. Englund, D. Wang, H. Fujigaki, H. Sakai, C. M. Micklitsch, R. Ghirlando, G. Martin-Manso, M. L. Pendrak, D. D. Roberts, S. R. Durell and D. H. Appella, *Nat. Commun.*, 2012, **3**.
28. B. M. G. Janssen, E. H. M. Lempens, L. L. C. Olijve, I. K. Voets, J. L. J. van Dongen, T. F. A. de Greef and M. Merkx, *Chem. Sci.*, 2013, **4**, 1442-1450.
29. S. Rinker, Y. Ke, Y. Liu, R. Chhabra and H. Yan, *Nat. Nanotechnol.*, 2008, **3**, 418-422.
30. L. E. Olesen, M. G. J. Ford, E. M. Schmid, Y. Vallis, M. M. Babu, P. H. Li, I. G. Mills, H. T. McMahon and G. J. K. Praefcke, *J. Biol. Chem.*, 2008, **283**, 5099-5109.
31. K. Walther, M. K. Diril, N. Jung and V. Haucke, *Proc. Natl. Acad. Sci. USA*, 2004, **101**, 964-969.
32. F. Diezmann, H. Eberhard and O. Seitz, *Biopolymers*, 2010, **94**, 397-404.
33. P. E. Nielsen, M. Egholm, R. H. Berg and O. Buchardt, *Science*, 1991, **254**, 1497-1500.
34. M. Egholm, O. Buchardt, L. Christensen, C. Behrens, S. M. Freier, D. A. Driver, R. H. Berg, S. K. Kim, B. Norden and P. E. Nielsen, *Nature*, 1993, **365**, 566-568.
35. M. Eriksson and P. E. Nielsen, *Nat. Struct. Biol*, 1996, **3**, 410-413.
36. V. M. Krishnamurthy, V. Semetey, P. J. Bracher, N. Shen and G. M. Whitesides, *J. Am. Chem. Soc.*, 2007, **129**, 1312-1320.
37. N. Kahlfeldt, A. Vahedi-Faridi, S. J. Koo, J. G. Schafer, G. Krainer, S. Keller, W. Saenger, M. Krauss and V. Haucke, *J. Biol. Chem.*, 2010, **285**, 2734-2749.